THE JOURNAL OF BIOLOGICAL CHEMISTRY
Vol. 279, No. 11, Issue of March 12, pp. 10185–10194, 2004
© 2004 by The American Society for Biochemistry and Molecular Biology, Inc.
Printed in U.S.A.

Thermal Stability and Aggregation of *Sulfolobus solfataricus* β-Glycosidase Are Dependent upon the *N*-ε-Methylation of Specific Lysyl Residues

CRITICAL ROLE OF *IN VIVO* POST-TRANSLATIONAL MODIFICATIONS*

Received for publication, August 4, 2003, and in revised form, December 2, 2003
Published, JBC Papers in Press, December 3, 2003, DOI 10.1074/jbc.M308520200

Ferdinando Febbraio‡§, Annapaola Andolfo¶, Fabio Tanfani‖, Raffaella Briante‡, Fabrizio Gentile‡‡, Silvestro Formisano§§, Carlo Vaccaro‡, Andrea Scirè‖¶¶, Enrico Bertoli‖¶¶, Piero Pucci¶‖‖, and Roberto Nucci‡**

*From the ‡Institute of Protein Biochemistry, CNR, Via Marconi 10, 80125 Napoli, Italy, ¶CEINGE Advanced Biotechnologies scarl, Via Pansini 5, 80131 Napoli, Italy, ‖Institute of Biochemistry, ¶¶Faculty of Medicine and Surgery, and **Faculty of Sciences, Polytechnical University of Marche, Via Ranieri, 60131 Ancona, Italy, ‡‡Department SAVA, University of Molise, Via De Sanctis, 86100 Campobasso, Italy, the §§Department of Cell and Molecular Biology and Pathology, University of Naples "Federico II" and Institute of Experimental Endocrinology and Oncology, CNR, Via Pansini 5, 80131 Napoli, Italy, and the ‖‖Department of Organic and Biological Chemistry, University of Naples "Federico II," Via Cinthia, 80126 Napoli, Italy*

Methylation *in vivo* is a post-translational modification observed in several organisms belonging to eucarya, bacteria, and archaea. Although important implications of this modification have been demonstrated in several eucaryotes, its biological role in hyperthermophilic archaea is far from being understood. The aim of this work is to clarify some effects of methylation on the properties of β-glycosidase from *Sulfolobus solfataricus*, by a structural comparison between the native, methylated protein and its unmethylated counterpart, recombinantly expressed in *Escherichia coli*. Analysis by Fourier transform infrared spectroscopy indicated similar secondary structure contents for the two forms of the protein. However, the study of temperature perturbation by Fourier transform infrared spectroscopy and turbidimetry evidenced denaturation and aggregation events more pronounced in recombinant than in native β-glycosidase. Red Nile fluorescence analysis revealed significant differences of surface hydrophobicity between the two forms of the protein. Unlike the native enzyme, which dissociated into SDS-resistant dimers upon exposure to the detergent, the recombinant enzyme partially dissociated into monomers. By electrospray mapping, the methylation sites of the native protein were identified. A computational analysis of β-glycosidase three-dimensional structure and comparisons with other proteins from *S. solfataricus* revealed analogies in the localization of methylation sites in terms of secondary structural elements and overall topology. These observations suggest a role for the methylation of lysyl residues, located in selected domains, in the thermal stabilization of β-glycosidase from *S. solfataricus*.

Post-translational modifications expand the cellular repertoire of proteins far beyond the possibilities offered by the 20 encoded amino acids, constituting one of the most exciting frontiers in modern biology. A little more than a dozen post-translational protein side-chain modifications have been identified so far.

Protein methylation occurs ubiquitously in nature, in bacteria, archaea, and eucarya, involving the amino groups of such residues as arginine, lysine, histidine, alanine, proline, and glutamine and hydroxyl groups of glutamic and aspartic acid (1). Methylated amino acids occur in highly specialized proteins, exerting diverse functional and structural roles, such as histones, flagellar proteins, myosin, actin, ribosomal proteins, opsin, EF-1α, HnPNP protein, HMG-1 and -2 proteins, fungal and plant cytochrome *c*, myelin basic protein, EF-Tu, heat shock proteins, calmodulin, etc. (1). The effects of methylation on the recruitment of heterochromatin proteins to specific histones in nucleosome cores and the subsequent effects on gene expression have been documented in detail (2). It was reported that methylation of the histone H3 tail is an epigenetic mark, affecting acetylation and phosphorylation of histone tail residues in mammals and *Drosophila* (3, 4). A model was suggested, in which the concerted deacetylation and methylation of Lys^9 of histone H3 led to a permanent silencing of transcription in particular areas of the genome (4). Methylation created a high affinity binding site for heterochromatin protein 1 (5, 6), which dimerized and thereby promoted the formation of higher order structures (7). In addition, histone methylation affected DNA methylation in the heterochromatin of *Neurospora crassa* (8).

The essential role of lysine methylation was demonstrated also in rat ribosomal proteins (9) and in the pathogenesis of late infantile ceroid lipofuscinosis (10). A recent observation of high medical interest concerns the inhibition of toxicity of the synthetic β-amyloid peptide β-(25–35) by *N*-methylation (11).

The presence of methylated lysyl residues has also been reported for proteins from thermophilic microorganisms, such as ferredoxin from the thermoacidophilic archaeon *Sulfolobus acidocaldarius* (12), and a number of proteins from the hyperthermophilic archaeon *Sulfolobus solfataricus* (13–15). In this regard, it has been shown that the rate constant of thermoinactivation of an enzyme is an inverse function of the number of modified ε-amino groups (16). However, no systematic study of the effect and nature of *N*-ε-methylation on the structural and

* This work was supported by a grant from the Ministero dell'Istruzione e della Ricerca Scientifica (MIUR) PRIN99 and PRIN01 projects (to F. T. and E. B.) and by a grant from the National Research Council (Rome, Italy). The costs of publication of this article were defrayed in part by the payment of page charges. This article must therefore be hereby marked "*advertisement*" in accordance with 18 U.S.C. Section 1734 solely to indicate this fact.

§ To whom correspondence should be addressed. Tel./Fax: 39-0817257300; E-mail: f.febbraio@ibp.cnr.it.

catalytic properties of thermophilic enzymes has been carried out.

β-Glycosidase from *S. solfataricus* (*Ss*βgly)[1] has been recently subjected to a detailed analysis of the structural determinants of protein stability, prompted by its peculiar behavior in the presence of SDS (17). This protein may also be adequate as a model for investigating the structural and functional consequences of *N*-ϵ-methylation of lysyl residues in archaea.

In the present study, a detailed structural characterization of the native, methylated *Ss*βgly and the unmethylated enzyme, recombinantly expressed in *Escherichia coli* (*Ec Ss*βgly) (18), was carried out. In order to discriminate between the different behaviors of the methylated and unmethylated forms of the protein, their thermal denaturation was investigated by Fourier transform infrared (FT-IR) spectroscopy and turbidimetry. The effects of methylation on protein stability in SDS were also investigated. Methylated residues were localized within the sequence by mass spectrometry. Moreover, the localization of methylation sites was analyzed in relation with neighboring elements of secondary structure and with the overall topology of the enzyme and also in relation with the pattern of sequence conservation between *Ss*βgly and other mesophilic β-glucosidases belonging to glycosyl hydrolase family I.

EXPERIMENTAL PROCEDURES

Materials—*S. solfataricus* strain MT4, isolated from acidic hot springs at Pozzuoli (Naples), was grown aerobically at 87 °C and pH 3.0 in a 100-liter fermenter, as previously described (19). Homogeneous *Ss*βgly (20) and *Ec Ss*βgly (18) were purified as described. Cyanogen bromide was purchased from Pierce. Trypsin was from Sigma, and endoproteases Glu-C, Asp-N, and Lys-C were obtained from Roche Molecular Biochemicals. Deuterium oxide (99.9%, $[^2H]_2O$) was purchased from Aldrich. All other reagents and solvents were of the highest purity. The high pressure liquid chromatography (HPLC) systems were from Hewlett Packard and Waters. The Nile Red and the standard of *N*-ϵ-methyl-L-lysine were from Sigma. The AccQ·Tag kit for amino acid analysis was from Waters.

Amino Acid Composition Analysis—Aliquots of homogeneous samples of *Ss*βgly were desalted by reverse phase HPLC on a Sephasil C_4 (5-μm) column and lyophilized in pyrolyzed glass tubes at 500 °C. Amino acid composition was determined on samples hydrolyzed in 6 N HCl at 153 °C for 1 h in sealed vials under vacuum. The sample was lyophilized and suspended in 20 mM HCl and derivatized using the AccQ·Fluor reagent kit (Waters), as described in the AccQ·Tag Method (Waters). Aliquots of derivatized samples were injected in a Breeze HPLC system (Waters) on an AccQ·Tag amino acid analysis (high efficiency Nova-Pak™ C_{18}; 4 μm) column (Waters), specifically certified for use with the AccQ·Tag method. The elution gradient in the AccQ·Tag Method was slightly modified in order to separate peaks of derivatized standards of L-leucine (retention time 33.3 min) and *N*-ϵ-methyl-L-lysine (retention time 33.6 min).

Preparation of Samples for Infrared Measurements—Typically, 1–1.5 mg of homogeneous native or recombinant protein, dissolved in the buffer used for their purification (20), were centrifuged in 30K centricon microconcentrators (Amicon) at 3000 × *g* and 4 °C and concentrated to a volume of ~40 μl. Then 300 μl of 50 mM phosphate buffer, p^{2}H 7.0, in $[^2H]_2O$, were added, and the samples were concentrated again. The p^{2}H value corresponds to the pH meter reading + 0.4 (21). This procedure was repeated several times in order to replace completely the original buffer with the phosphate buffer. In the last washing, the protein samples were concentrated to a final volume of 40 μl and used for the infrared measurements. The time of contact of the proteins with the $[^2H]_2O$ medium prior to FT-IR analysis was about 24 h. At least three different measurements were carried out on different samples of each protein.

Infrared Spectra—The concentrated homogeneous protein samples were placed in a thermostatted Graseby Specac 20500 cell (Graseby-Specac Ltd., Orpington, Kent, UK) fitted with CaF_2 windows and 25-μm Teflon spacers. FT-IR spectra were recorded by means of a PerkinElmer Life Sciences 1760-x Fourier transform infrared spectrometer, using a deuterated triglycine sulfate detector and a normal Beer-Norton apodization function. At least 24 h before and during data acquisition, the spectrometer was continuously purged with dry air at a dew point of −40 °C. Spectra of buffers and samples were acquired at 2-cm^{-1} resolution, under the same scanning and temperature conditions. Typically, 256 scans were averaged for each spectrum obtained at 20 °C, whereas 32 scans were averaged for spectra obtained at higher temperatures. In the thermal denaturation experiments, the temperature was raised by 5 ± 0.1 °C steps from 20 to 95 °C. Before acquiring spectra, samples were maintained at the desired temperature for the time necessary for the stabilization of temperature inside the cell (6 min). Spectra were collected and processed using the Spectrum software from PerkinElmer. The deconvoluted parameters for the amide I band were set with a γ value of 2.5 and a smoothing length of 60.

Turbidimetric Measurements—Samples containing 250 μg/ml homogeneous *Ss*βgly or *Ec Ss*βgly in 50 mM sodium phosphate buffer, pH 7.0, were filtered on 0.22-μm sterile filters (Millipore Corp.). Absorbances were recorded in a 1-cm light path quartz cuvette, at a wavelength of 600 nm, using a spectrophotometer Cary 1E thermostatted with a Cary temperature controller accessory, equipped with a Peltier's heat exchange device positioned around the sample, with an error of 0.1 °C. The temperature was increased from 50 to 95 °C at a rate of 1 °C/min, and the increase in absorbance at 600 nm was recorded. At least three different measurements were carried out on different samples and at different concentrations.

Thermal Stability Measurements—The thermal stability of *Ss*βgly and *Ec Ss*βgly was measured by incubating a 0.41 μM concentration of the homogeneous enzyme in 0.1 M sodium phosphate buffer, pH 6.5, at 85 °C in a thermostatted water bath. At time intervals, aliquots containing 4.1 pmol of the enzyme were withdrawn from the incubation mixture and assayed at 75 °C under the conditions described (20).

Nile Red Fluorescence—All analyses were performed with a Jasco FP777 spectrofluorimeter, thermostatted at room temperature, using cells with a working volume of 500 μl and a path length of 10 mm. The excitation wavelength was set at 550 nm, and excitation and emission slits were set at 5 and 10 nm, respectively. Nile Red (0.25 mM in Me_2SO) was added in the cuvette containing homogeneous samples of 0.41 μM *Ss*βgly or *Ec Ss*βgly, up to a final concentration of 1 μM, and spectra were recorded after 15 min. In a hydrophobic environment, a blue shift in the maximum emission wavelength (about 665 nm in water) and an increase in the fluorescence intensity of Nile Red are observed.

Preparation of Linear Transverse Gradient Polyacrylamide Gels—The preparation of linear transverse-gradient polyacrylamide gels was described in detail (17). Linear transverse gradient gels were used, containing 4–9% total acrylamide from left to right, 2.7% *N,N′*-methylene bis-acrylamide, in 0.375 M Tris/HCl, pH 8.8, 0.1% SDS, polymerized on a sheet of GelBond-PAG (Bio-Whittaker). No stacking gel was used, but a sample gel containing 3.75% total acrylamide in electrode buffer was created on top of the gel. Reference standards and *Ss*βgly or *Ec Ss*βgly were subjected to electrophoresis all together in alternate lanes of 20-lane gels. The electrode buffer contained 0.025 M Tris base, 0.19 M glycine, pH 8.2, 0.1% SDS. The enzymes were dissolved in 0.01 M Tris/HCl, pH 6.8, 1% SDS, 0.7 M β-mercaptoethanol, 1.36 M glycerol, and 0.005% bromphenol blue as tracking dye. SDS electrophoresis was conducted at 15 °C at 10 mA, until the dye front reached the lower end on the left side of the gels. The gels were stained with Coomassie Brilliant Blue R-250.

Molecular Mass Estimation by Ferguson Analysis of Linear Transverse Gradient Polyacrylamide Gels—The molecular mass of *Ss*βgly and *Ec Ss*βgly was determined as described (17), by indirect comparison of the relative mobilities (R_m) of the enzyme and those of calibration proteins, after electrophoresis in a linear transverse gradient polyacrylamide gel. A detailed description of the method was reported (17).

Chemical and Enzymatic Hydrolyses—Homogeneous β-glycosidase samples were digested by CNBr in 70% trifluoroacetic acid, at room temperature, for 18 h in the dark. Samples were diluted with 4 volumes of distilled H_2O and lyophilized. CNBr fragments were purified by HPLC on a Vydac C_4 column (25 × 0.46 cm; 5 μm), using 0.1% trifluoroacetic acid (solvent A) and 0.07% trifluoroacetic acid in 95% acetonitrile (solvent B), by means of a two-step gradient. The column was equilibrated at 20% of solvent B for 5 min, and then the acetonitrile concentration was raised from 20 to 35% in 15 min and from 35 to 60% in 33 min. The elution was monitored at 220 and 280 nm.

Selected CNBr peptides from *Ss*βgly were subdigested overnight at

[1] The abbreviations used are: *Ss*βgly, *S. solfataricus* β-glycosidase; *Ec Ss*βgly, *S. solfataricus* β-glycosidase recombinantly expressed in *E. coli*; *Ss*ADH, *S. solfataricus* alcohol dehydrogenase; FT-IR, Fourier transform infrared; HPLC, high performance liquid chromatography; ES-MS, electrospray mass spectrometry; MALDI, matrix-assisted laser desorption ionization; amide I′, amide I band in a $[^2H]_2O$ medium; ES, electrospray; MS, mass spectrometry.

37 °C with endoproteinase Asp-N in 0.4% ammonium bicarbonate containing 10% acetonitrile, pH 8.5, using an enzyme-to-substrate ratio of 1:100 (w/w). Subdigestion of the peptide mixtures by endoproteinase Glu-C, trypsin, or endoproteinase Lys-C was carried out in 50 mM ammonium bicarbonate, pH 8.5, for 18 h at 37 °C, using an enzyme-to-substrate ratio of 1:50 (w/w). Under the alkaline conditions used for the enzymatic digestions, the C-terminal lactone of each CNBr fragment was hydrolyzed to free homoserine. Samples were then lyophilized twice prior to matrix-assisted laser desorption ionization (MALDI) mass spectrometry.

Mass Spectrometry—Intact homogeneous proteins or individual peptide fractions were submitted to electrospray mass spectrometry (ES-MS), using a BIO-Q triple quadrupole mass spectrometer (Micromass). Samples were dissolved in 1% acetic acid in 50% acetonitrile, and 2–10 μl were injected into the mass spectrometer at a flow rate of 10 μl/min. The quadrupole was scanned from *m/z* 600 to 1800 at 10 s/scan, and the spectra were acquired and elaborated using the MassLynx software (Micromass). Calibration was performed with the multiply charged ions from a separate injection of myoglobin (M_r = 16,951.5). All mass values are reported as average masses.

MALDI mass spectra were recorded using a Voyager DE MALDI-time-of-flight mass spectrometer (Applied Biosystems). A mixture of analyte solution, α-cyano-4-hydroxycinnamic acid, and bovine insulin was applied to the sample plate and air-dried. Mass calibration was performed using the molecular ions from bovine insulin at 5734.6 and a matrix peak at 379.1 as internal standards. Raw data were analyzed with a computer software provided by the manufacturer and were reported as average masses.

Computational Analysis—All structure calculations were performed on a SGI IRIS O_2 R10000 computer. Our simulations were based on the crystal structure of *Ss*β-gly refined at 2.6 Å (Protein Data Bank entry 1GOW) (22).

Lysines 116, 135, 273, 311, and 332 were modified, using the Biopolymer module implemented in InsightII 98.0 (Biosym/MSI) (23), by the addition of a methyl group, from the InsightII library, to the side chain N^{ϵ} atom. In the same module, hydrogen atoms were added to the methylated and unmethylated protein structures at pH 7.0. The cvff force field was applied to the two structures, and the resulting protonated state of the modified and unmodified protein gave a total charge of −36. The positions of the side chains were optimized by subsequent molecular mechanics calculations, using the Discover 3 module implemented in InsightII 98.0 (Biosym/MSI) (23). For the minimization process, a conjugate gradient was applied after 50 steps of steepest descent algorithm. After minimization, the differences in the *N*-ϵ-methyl-lysine area were analyzed by the Viewer module of InsightII 98.0. The exposed solvent surfaces of the modified and unmodified proteins were calculated using the Molmol program, release 2.5 (24), with a standard radius of 1.4 Å.

Comparisons between the sequences of β-glycosidase (Swiss-Prot accession number P22498) (25), alcohol dehydrogenase (*Ss*ADH) (Swiss-Prot accession number P39462) (13), aspartate aminotransferase (pir accession number S07088) (26), and glutamate dehydrogenase (pir accession number S20286) (14) from *S. solfataricus* were performed using ClustalX (27). Structure comparisons between *Ss*β-gly (Protein Data Bank accession number 1GOW) (22) and *Ss*ADH (Protein Data Bank accession number 1JVB) (28) were performed using Swisspdb viewer 3.7 (29). The analysis of *Ss*β-gly and *Ss*ADH structural topology was obtained using the TOPS (topology of protein structure) software available on the World Wide Web at www.tops.leeds.ac.uk/ (30).

RESULTS

Organism and Growth—Sulfolobus solfataricus strain MT-4, isolated from acidic hot springs at Pozzuoli (Naples), was grown *in vitro* in a 100-liter fermenter (19), in strict accordance with the optimal conditions described for growth *in vivo* (*i.e.* at 87 °C and pH 3.0, in aerobiosis) (31). The yield of bacterial biomass was about 240–280 g per 100 liters of culture broth.

Amino Acid Composition Analysis—Several aliquots of homogeneous *Ss*β-gly from different growth cycles of *S. solfataricus* were analyzed for their amino acid composition. The relative content of methylated lysines resulting from the analyses was between 14 and 17% (data not shown). Considering that 5 lysines of 23 (21.7%) were methylated (see below), these results indicated a constantly substoichiometric level of modification in the *in vitro* culture.

FT-IR Spectroscopy—In the FT-IR deconvolution spectra of Ssβ-gly and *Ec*Ssβ-gly at p^2H 7.0, the amide I′ bands (1700–1600-cm^{-1} region) of the two β-glycosidase forms were almost indistinguishable, which indicates nearly identical secondary structure contents for the two forms of the protein. Only small differences were noticed, by monitoring the amide I′ bandwidth as a function of the temperature (32, 33) at p^2H 7.0, in order to determine the thermal denaturation curves of the two forms of the protein (data not shown). Since this method did not appear to be sufficiently sensitive to detect subtle changes in the secondary structure, a more detailed investigation of protein thermal denaturation was performed by difference spectroscopy (32, 34, 35). Difference spectra were derived from the series of spectra recorded at stepwise increasing temperatures, by subtracting each one of them from the spectrum recorded at the next higher temperature. For example, the 95 – 90 °C difference spectrum corresponded to the spectrum recorded at 95 °C, after subtraction of the one recorded at 90 °C. In these spectra, a negative band indicated a lower content of a particular secondary structural element in the spectrum recorded at higher temperature and *vice versa* (Fig. 1, *A* and *B*). Hence, the negative broad band between 1600 and 1700 cm^{-1} corresponded to the loss of secondary structure in the sample recorded at higher temperature (34), whereas the two positive peaks close to 1617 and 1685 cm^{-1} represented protein aggregation brought about by thermal denaturation (34). The negative band close to 1540 cm^{-1} mainly represented an enhanced $^1H/^2H$ exchange, caused by the increase of temperature and by protein unfolding (36). The difference spectra of native and recombinant proteins, shown in Fig. 1, *A* and *B*, indicated the onset of protein denaturation and aggregation. In particular, the small negative band at 1657.2 cm^{-1} represented a partial loss of α-helices in the samples assayed at higher temperature, whereas the positive peak close to 1617 cm^{-1} reflected protein aggregation. From these spectra, it appears that protein aggregation paralleled protein denaturation. The amplitudes of the negative and positive bands in the 94.2 – 89.0 °C difference spectrum of *Ss*β-gly were smaller than those present in the corresponding difference spectrum of *Ec*Ssβ-gly. Moreover, the T_m was observed in the 99.0 − 98.1 °C spectrum for native *Ss*β-gly and in the 98.1 − 97.2 °C spectrum for *Ec*Ssβ-gly (Fig. 1, *A* and *B*).

When the normalized absorbance values of the broad negative band between 1600 and 1700 cm^{-1} and of the positive peak close to 1617 cm^{-1}, reflecting denaturation and aggregation, respectively, were divided by the corresponding temperature increments, the Δ*A*/°C was obtained. This is the rate of change of the absorbance as a function of the temperature and represents a measure of the total changes in a particular peak (35, 37). The plots of Δ*A*/°C *versus* temperature for the native and the recombinant proteins are shown in Fig. 1*C*. The negative and positive profiles are related to protein thermal denaturation and aggregation, respectively. The process of denaturation/aggregation of *Ec*Ssβ-gly attained significant levels already in the 89–94 °C interval (see also the difference spectrum 94.2 − 89.0 °C) and steadily progressed up to 99 °C, whereas in *Ss*β-gly it was only marginal between 89 and 94 °C and concentrated in the 94–99 °C interval. These data demonstrate that, although the temperature of onset of denaturation was the same in both samples, the progression of unfolding was different, *Ss*β-gly being more resistant toward denaturation than *Ec*Ssβ-gly.

Turbidimetry—Measurements of the absorbance at 600 nm, as a function of temperature, were performed in order to obtain information on the protein aggregation process. Fig. 2*A* shows the increase in absorbance of homogeneous *Ss*β-gly and

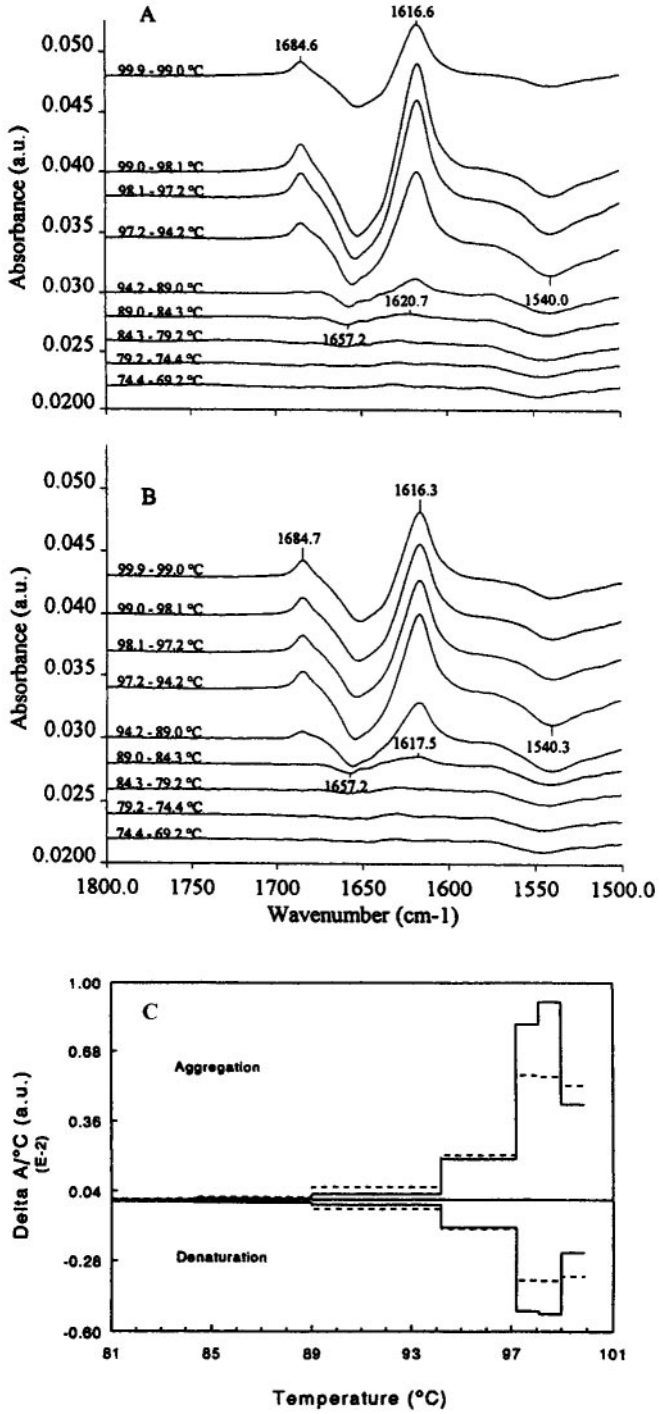

FIG. 1. **FT-IR spectroscopy.** Difference spectra of *Ss*βgly (*A*) and *EcSs*βgly (*B*) were derived from the series of IR spectra recorded at stepwise increasing temperatures, by subtracting each one of them from the spectrum recorded at the next higher temperature. *C*, plot of Δ*A*/°C *versus* temperature. *Continuous line*, *Ss*βgly; *dashed line*, *EcSs*βgly. Negative and positive profiles reflect protein denaturation and aggregation, respectively.

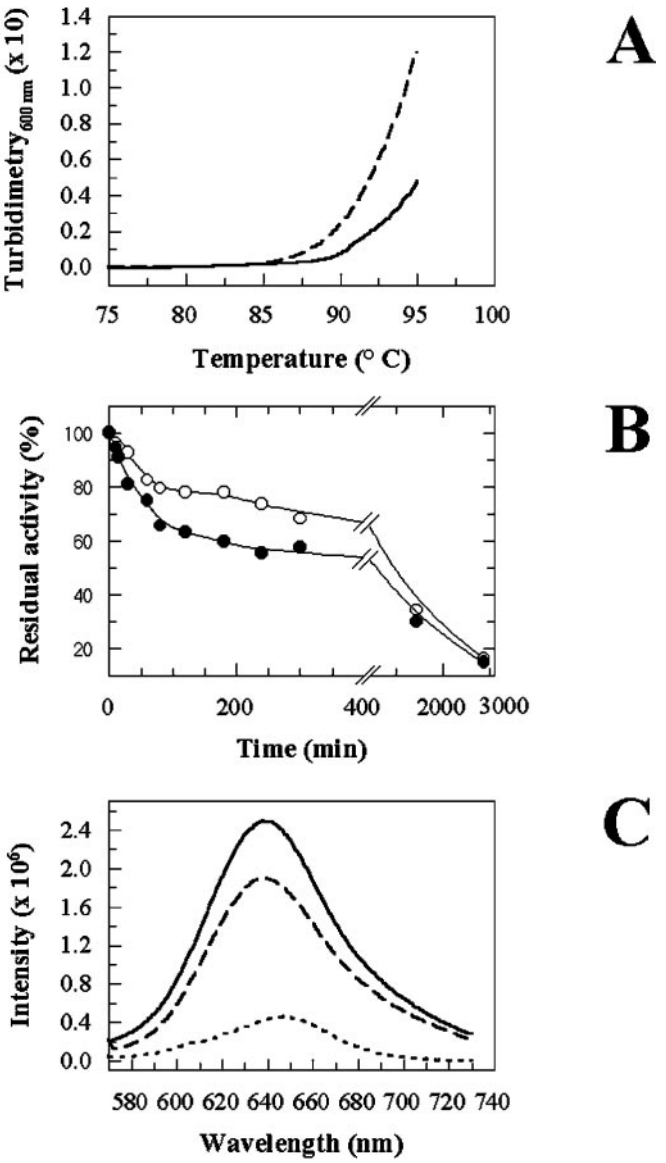

FIG. 2. *A*, turbidimetry. Aggregation was monitored by measuring the absorbance of native and recombinant protein samples at 600 nm, as a function of temperature, in the range 75–95 °C. *Continuous* and *dashed lines* represent *Ss*βgly and *EcSs*βgly, respectively. *B*, analysis of thermal stability. Plot of the residual activity measured at 75 °C, after exposure to 85 °C for the time indicated. *Empty circles*, *Ss*βgly; *filled circles*, *EcSs*βgly. C, Nile Red fluorescence. The excitation wavelength was set at 550 nm, and emission spectra were recorded in the range 570–740 nm. *Continuous*, *dashed*, and *dotted lines* represent *Ss*βgly, *EcSs*βgly, and Nile Red alone in buffer, respectively.

*EcSs*βgly solutions in the temperature range 75–95 °C. As to the temperature of melting, only the onset of the process could be comparatively observed with the two forms of the enzyme, due to the limitations of the technique at high temperatures. The two spectra showed that aggregation started at about 85 °C for the recombinant enzyme and at about 90 °C for the native enzyme, indicating a hindrance by methylated lysyl residues in the development of protein aggregates.

Thermal Stability Measurements—In the comparative assay of the thermal stability of *Ss*βgly and *EcSs*βgly at 85 °C (Fig. 2*B*), the trend of the residual enzymatic activity was characterized by an initial phase of exponential decay, during which the activity of *EcSs*βgly reached levels, in about 40 min, that were attained by *Ss*βgly only after more than 5 h. It was followed by a phase of slower decay, during which the recombinant enzyme exhibited values of residual activity uniformly lower than those of the native enzyme.

Nile Red Fluorescence—Nile Red is nearly insoluble in water and is adsorbed onto plastic, glass, or quartz, when added to an aqueous buffer solution. In so doing, it becomes nonfluorescent. Its half-life is about 20–25 min in distilled water, whereas it is about 11 min in the presence of various buffers (Tris, phosphate, imidazole). On the other hand, its binding to proteins is

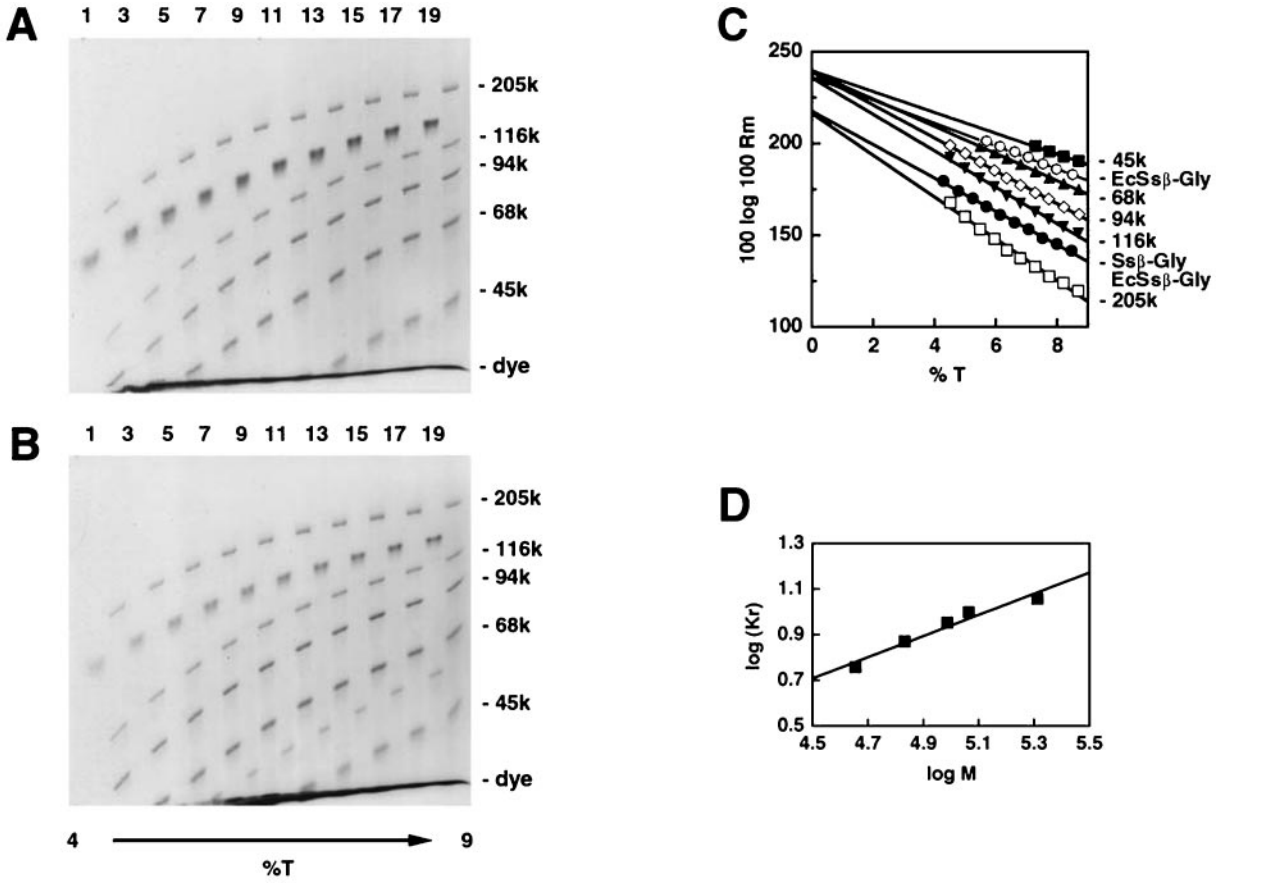

FIG. 3. **Ferguson analysis of the polyacrylamide gel electrophoresis in SDS of *Ssβ*gly and *EcSsβ*gly.** 4–9% T (total acrylamide) transverse gradient gels used for the determination of the molecular mass of *Ssβ*gly (*A*) and *EcSsβ*gly (*B*) in 0.1% SDS. The *image* in *A* is taken from Ref. 10. Acrylamide concentration increased from the *left* to the *right* side of the gels. *Odd lanes* (*numbered* at the *top*) contained 2.5 μg each of *Ssβ*gly (*A*) or *EcSsβ*gly (*B*), whereas *even-numbered lanes* contained molecular mass standards (2 μg each), marked at the *right side* of each gel. The dye front is indicated. *C*, Ferguson plot constructed on the base of the gels in *A* and *B* for the set of reference proteins and the molecular species of *Ssβ*gly and *EcSsβ*gly. *D*, plot of the log of measured K_r *versus* log *M* of the reference proteins used to interpolate the log *M* of the molecular species of *EcSsβ*gly.

very fast and stable (maximum fluorescence with β-lactoglobulin is reached within 3 s of mixing and decreases by less than 4% in 4 h) (38). Its high excitation wavelength also prevents absorption interference from proteins or cofactors, and the significant Stokes' shifts observed in emission wavelength allow the detection of small changes in protein structure. These properties make Nile Red a useful probe of hydrophobic sites in many native proteins (38). The spectra of homogeneous *Ssβ*gly and *EcSsβ*gly in the presence of Nile Red (Fig. 2*C*) showed blue shifts at about 637 and 638 nm, respectively. Instead, the increase in fluorescence intensity was larger in the native, methylated protein, indicating patches with increased hydrophobicity on the protein surface.

Determination of the Molecular Mass of β-Glycosidase by Ferguson Plot-based Analysis of Polyacrylamide Gels in SDS—For the determination of the molecular mass of *Ssβ*gly and *EcSsβ*gly, the two forms of the enzyme and a set of reference proteins, ranging in molecular mass from 45,000 to 205,000, were subjected to electrophoresis in Tris/glycine according to Laemmli (39), in the presence of 0.1% SDS, on two 4–9% total acrylamide, 2.7% *N*,*N*′-methylene bisacrylamide transverse gradient gels (Fig. 3, *A* and *B*). At the end of electrophoresis, a Ferguson plot was constructed, and the mass of the enzyme was determined, using the function 100 log 100 R_m *versus* log *M* (Fig. 3, *C* and *D*). By using this technique, we have previously documented that *Ssβ*gly in 0.1–1% SDS dissociates incompletely into dimers, whose relative molecular mass was estimated around 109,400 (17). In order to test the impact of the lack of post-translational modifications on the behavior of *EcSsβ*gly in SDS, we performed the analogous analysis with the recombinant enzyme. Comparison between *A* and *B* of Fig. 3 revealed an additional molecular species in *EcSsβ*gly, for which a mass of about 52000 was estimated, thus deriving from the partial dissociation of *EcSsβ*gly into monomers. The relative abundance of this species was estimated as being 25% of total protein by densitometry.

Analysis of Sulfolobus Solfataricus β-Glycosidase by Mass Spectrometry—An aliquot of homogeneous *Ssβ*gly was desalted by reverse phase HPLC and directly analyzed by ES-MS. The spectrum obtained showed the characteristic bell-shaped distribution of multiple charged ions, from which a relative molecular mass of 56,754.8 ± 4.9 was calculated. The multiple charged ion spectrum was then transformed onto a real mass scale (Fig. 4*A*). The measured mass value was slightly larger than predicted for *Ssβ*gly (M_r = 56,690.7), suggesting the occurrence of post-translational modifications. The protein was then submitted to a detailed structural investigation, by employing the ES-mapping strategy developed for the analysis of medium/large-sized proteins (15, 40). An aliquot of *Ssβ*gly was digested with CNBr, and the resulting peptide mixture was fractionated by HPLC. A two-step gradient procedure was developed, which led to the separation of all CNBr peptides in a single chromatographic step, with the exception of peptides CB10 and CB11 (Fig. 4*B*). Individual CNBr peptides were manually collected, and their molecular masses were accurately determined by direct ES-MS analysis of the HPLC frac-

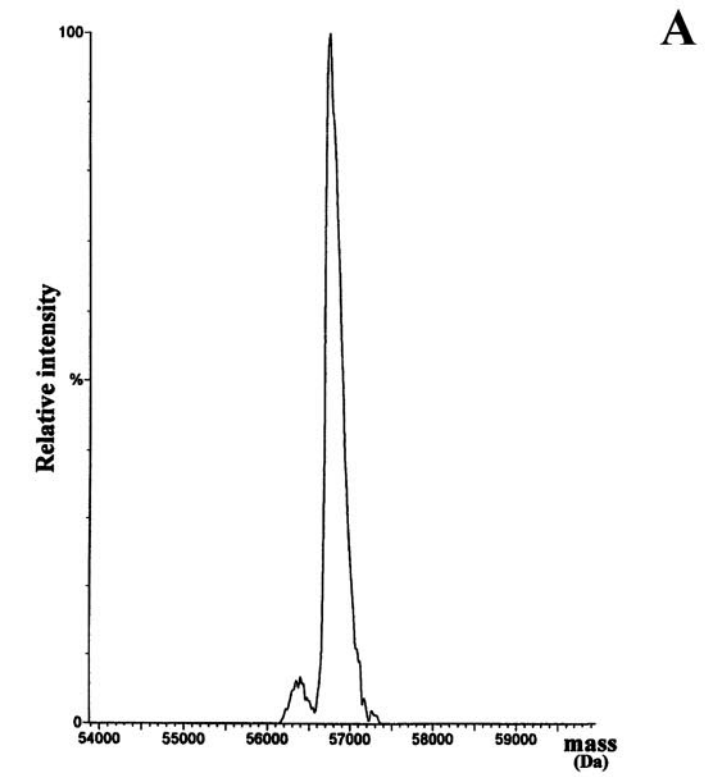

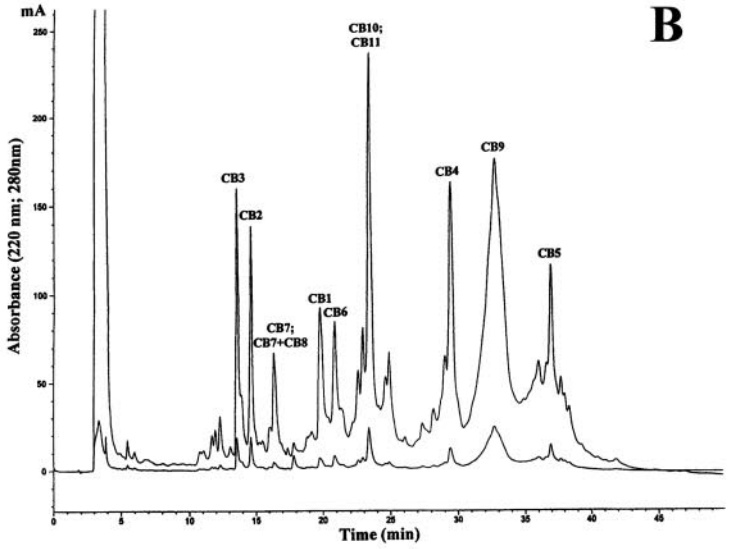

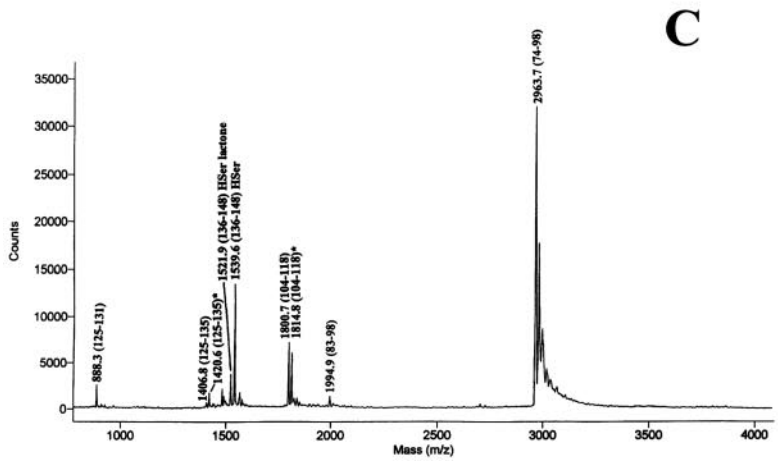

FIG. 4. **Mass spectrometry.** *A*, electrospray mass spectrum of *Ssβ*gly. The mass signal was transformed onto a real mass scale. *B*, HPLC chromatogram of the CNBr peptides from *Ssβ*gly. The CNBr fragments are numbered according to their order along the *Ssβ*gly sequence. *C*, MALDI-MS spectrum of *Ssβ*gly CB4 subdigested with endoproteinase Asp-N. Each mass signal was assigned to the corresponding peptide (in *parentheses*) on the basis of the theoretical molecular mass. The *asterisks* indicate the two peptides containing *N*-ϵ-methyl-lysines.

TABLE I
ES-MS of the CNBr peptides from Ssβgly
Modified fragments are shown in boldface type.

CNBr peptide	Measured molecular mass	Theoretical molecular mass	Modified lysines
CB1	2456.9 ± 0.3	2456.6	
CB2	2527.7 ± 0.2	2527.6	
CB3	3190.0 ± 0.1	3190.4	
CB4	8945.7 ± 0.9	8946.1	
	8962.2 ± 0.4		**116 or 135**[a]
	8976.2 ± 0.9		**116 and 135**[b]
CB5	6719.7 ± 0.7	6719.6	
CB6	3350.4 ± 0.6	3349.8[c]	
CB7	4292.2 ± 0.7	4292.9	
	4306.6 ± 0.4		**273**
CB7 + CB8	4822.2 ± 0.8	4822.4	
	4836.7 ± 0.5		**273**
CB9	12101.3 ± 1.4	12,103.5	
	12,117.6 ± 1.0		**311 or 322**[a]
	12,133.7 ± 1.0		**311 and 322**[b]
CB10	6425.9 ± 0.6	6424.9	
CB11	5848.7 ± 0.3	5848.8	

[a] In these molecular species, the addition of a single methyl group (mass difference = 14) indicated the modification of one or the other of the two lysyl residues identified in the corresponding molecular species (see Footnote *b*), bearing two additional methyl groups (mass difference = 28).
[b] Molecular species corresponding to those described in Footnote *a*.
[c] Theoretical molecular mass of the peptide with Ala at position 235.

tions. Table I reports the theoretical and measured mass values of the CNBr peptides. In all cases, the accuracy of the mass measurement was within 1.5 mass units of the theoretical value. The ES mapping procedure led to a rapid screening of the entire *Ss*βgly sequence and highlighted the occurrence of peculiar structural features. The ES-MS analysis of CB4, CB7, and CB9, in fact, revealed, together with the expected peptides, additional components having mass values 14 units larger. These species were identified as methylated forms of the peptides, resulting from post-translational modification of lysyl residues, according to a substoichiometric ratio (15). Each modified CNBr fragment was then subdigested with suitable proteolytic enzymes. The resulting peptide mixtures were directly analyzed by MALDI-MS, which led to the identification of the modification sites.

As an example, Fig. 4*C* shows the MALDI spectrum of peptide CB4 digested with endoproteinase Asp-N. Each mass signal was associated with the corresponding peptide on the basis of its mass value. The results are summarized in Table II. The signals at *m/z* 1800.7 and 1406.8, corresponding to peptides 104–118 and 125–135, respectively, were accompanied by 14 units larger satellite peaks. Since both fragments contained a single lysyl residue, the assignment of methylation sites at Lys^{116} and Lys^{135} was straightforward. These results were confirmed by the analysis of the Glu-C digest of CB4, showing that all of the other lysyl residues of this peptide (*i.e.* Lys^{76}, Lys^{102}, Lys^{124}, and Lys^{138}) were unmodified.

Analogously, subdigestion of CB7 and CB9 with trypsin, Asp-N, and Lys-C led to the identification of methylated lysyl residues at position 273 in the CB7 fragment and 311 and 332 in the CB9 peptide, confirming in all cases that the modification had occurred to a substoichiometric extent. From the analysis of different mass peaks relative to the methylated and unmethylated forms of lysyl residues, it appeared that only particular positions were methylated. In particular, Lys^{135} and Lys^{332} were essentially in the methylated form, whereas the lysyl residues at the other three positions were methylated according to a substoichiometric ratio.

Protein Sequence Mismatch—The molecular mass value measured for fragment CB6, spanning residues 205–236, was 3350.4 ± 0.6, about 67 units less than the value indicated in the published *Ss*βgly sequence (25). In order to identify the cause of such a variation, purified CB6 was subdigested with trypsin, and the resulting peptide mixture was directly analyzed by MALDI-MS. The analysis confirmed the sequence already determined for the subfragment of peptide CB6 spanning residues 205–233 and suggested that the putative amino acid variation had to be located between residues 234 and 236. A second aliquot of CB6 was incubated with carboxypeptidase A, the reaction mixture was sampled at different time intervals, and the various aliquots were analyzed by MALDI-MS. The mass shift of the peptide, following the consecutive removal of amino acids from the C terminus, unambiguously demonstrated the presence of Ala at position 235, instead of His, as deduced from the cDNA sequence (25), probably indicating an error of cDNA synthesis or sequencing. The sequence thus found was 100% homologous with the sequence determined for the β-glycosidase from *S. solfataricus* 98/2 plasmid-based *E. coli* expression library (41).

TABLE II
MALDI-MS of the CB4 peptide digested with endoproteinase Asp-N

MH^+	Peptide	Notes
888.3	125–131	
1406.8	125–135	
1420.6	125–135	*N*-ε-Methyl-Lys^{135}
1539.6	136–148	
1800.7	104–118	
1814.8	104–118	*N*-ε-Methyl-Lys^{116}
1994.9	83–98	
2963.7	74–98	

Analysis of E. coli Recombinant β-Glycosidase by Mass Spectrometry—The analysis of *EcSs*βgly by ES-MS indicated a mass value of 56690.3 ± 4.2, 67 units less than the theoretical molecular mass calculated previously (25), confirming the presence of an Ala residue instead of a His residue and ruling out the presence of any sort of post-translational modification.

The enzyme was then hydrolyzed with CNBr as described above, and the individual CNBr fragments, purified by HPLC, were analyzed by ES-MS. The mass spectral investigation confirmed that the *EcSs*βgly was totally devoid of post-translational modifications, as previously reported for another recombinant thermophilic protein (42).

Computational Analysis—The topology of modified lysyl residues in the *Ss*βgly structure was investigated, in a search for structural elements or motifs possibly associated with susceptibility to the methylation of lysyl residues. To this aim, we compared the neighboring structural elements of all five *N*-ε-methyl-lysyl residues of *Ss*βgly with each other and with those of *N*-ε-methyl-lysyl residues of *Ss*ADH. The latter is the only other *S. solfataricus* protein for which both the x-ray crystallographic structure was resolved at 1.85 Å (28) and the location of methylation sites (Lys^{11} and Lys^{213}) was determined (13). Interesting similarities in the topology of methylated sites were noticed. In both proteins examined, methylated lysyl residues occurred in β-turns between two β-sheets, or within α-helices. In particular, Lys^{116} and Lys^{135} of *Ss*βgly were located inside α-helices 112–118 and 124–140, respectively, at the four corners of the tetramer, whereas Lys^{273}, Lys^{311}, and Lys^{332} were located in β-turns 273–274, 308–312, and 331-332, respectively, in the proximity of the catalytic site tunnel (Fig. 5*A*).

In addition, the analysis of the structure indicated that the stoichiometry of methylation of the various lysyl residues was independent of their solvent surface exposure. In fact, although Lys^{273} and Lys^{116} had higher percentages of solvent-exposed surface areas (56.9 and 41.6%, respectively) than Lys^{135} and

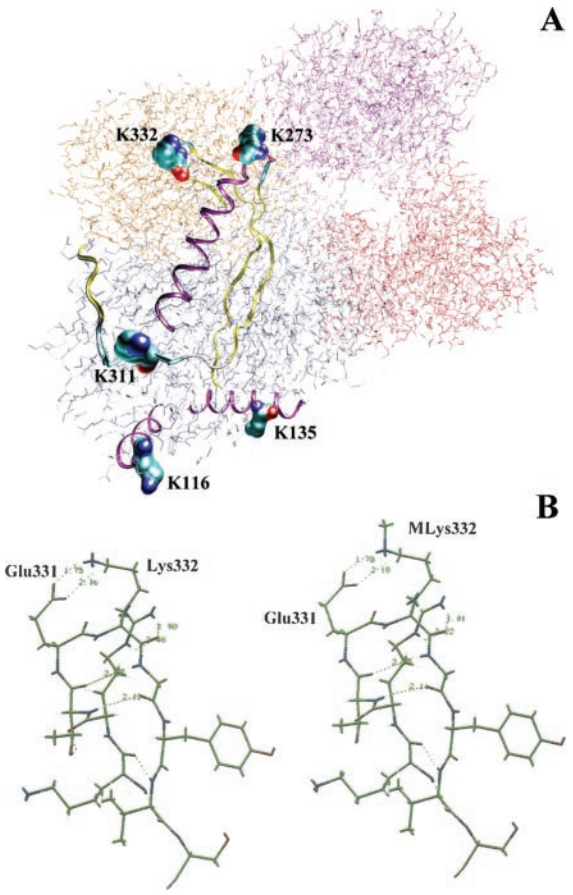

FIG. 5. **Distribution and hydrogen bonds of *N*-ε-methylated lysyl residues in the *Ssβ*gly structure.** *A*, perspective representation of the *Ssβ*gly tetramer (*transparent stick model*). The modified lysyl residues in the A subunit (*blue*) are in surface representation and *colored* in standard atom *colors*. Secondary structural elements near modified positions are in a *ribbon representation* and colored in *magenta*, *yellow*, and *green* for α-helix, β-sheet, and random coil structures, respectively. Subunits B, C, and D are in *magenta*, *red*, and *gold*, respectively. The image was realized using the VMD 1.7.2 program (54) in the POV format and rendered using the Pov-Ray™ version 3.1g program (Persistence of Vision™ Ray Tracer; the POV-Ray Team™; available on the World Wide Web at www.povray.org). *B*, changes in hydrogen bond distances (*dotted*) between methylated (*right*) and unmethylated (*left*) Lys^{332} and Glu^{331} after energy minimization. The *image* was realized using the InsightII program (Biosym/MSI).

Lys^{332} (37.9 and 39.1%, respectively), the latter residues were modified according to a nearly stoichiometric ratio, as mentioned above. Moreover, other nonmethylated lysyl residues (*e.g.* Lys^{219}, having 60.5% of solvent-exposed surface area) were more exposed on the protein surface than methylated residues. Sequence comparison between all *S. solfataricus* protein sequences with known methylation sites (*Ssβ*gly, *Ss*ADH, *S. solfataricus* aspartate aminotransferase, and *S. solfataricus* glutamate dehydrogenase) did not reveal any consensus for *N*-ε-methylation of lysines.

In order to explain the effect of methylated residues on enzyme stability, energy minimization calculations were performed on the crystal structure of the enzyme, to allow for the addition of methyl groups and to analyze their interactions with neighboring side-chain and backbone atoms. As usually observed in thermophilic proteins, all modified lysyl residues in *Ssβ*gly were involved in hydrogen and ionic bonds with other negatively charged residues on the protein surface, such as glutamyl and aspartyl residues, and were integrated in the ionic interaction network at the protein surface. The exploration of several energetic states of the protein globule, by different rounds of energy minimization, evidenced, in most cases, a reduction of the intermolecular distances for the methylated form of β-glycosidase, in comparison with the unmethylated form (Fig. 5*B*).

DISCUSSION

The present work documents that *N*-ε-methylated β-glycosidase from *S. solfataricus* is characterized by a higher resistance to aggregation and denaturation at physiological pH, in comparison with the unmethylated form recombinantly expressed in *E. coli*, as indicated by FT-IR and turbidimetric analyses. FT-IR spectroscopy is a powerful technique for the study of protein secondary structure, whose high accuracy and reproducibility allow the detection of subtle changes and differences between structures (32, 33). This technique did not show differences of secondary structure content between the two forms of β-glycosidase investigated, in agreement with previous far and near UV CD spectra (18). This observation emphasizes the role of *N*-ε-methylation of lysyl residues in the functional and structural differences observed. In this regard, the comparative analysis of temperature perturbation of the methylated and unmethylated forms of the protein, monitored by FT-IR spectroscopy, evidenced significant differences in the progression of thermal denaturation (Fig. 1). In particular, native *Ssβ*gly exhibited a higher resistance than *EcSsβ*gly, which was reflected in its higher T_m. The narrower and higher temperature range in which most of the aggregation and denaturation of *Ssβ*gly occurred, in comparison with *EcSsβ*gly, suggests that the native enzyme was composed of a more homogeneous population of molecules, endowed with a more rigid and stable structure.

The susceptibility of the two forms of the protein to denaturation and aggregation induced by thermal perturbation was analyzed. Aggregation of *EcSsβ*gly was observed by turbidimetry at about 5 °C under the temperature required to induce the same phenomenon with *Ssβ*gly (Fig. 2*A*), thus confirming that significant modifications in the surface properties of the enzyme were brought about by the addition of methyl groups. In keeping with these results, Nile Red fluorescence measurements (Fig. 2*C*) revealed an increased hydrophobicity of the native enzyme, in comparison with the recombinant protein. This finding is consistent with the apolar nature of the added methyl groups. Interestingly, these structural differences between the two protein forms were reflected also in changes of their functional properties, such as the 23% decrease of the k_{cat}/K_m ratio of *EcSsβ*gly (18) and the faster decay of *EcSsβ*gly activity at 85 °C (Fig. 2*B*).

In order to investigate the possible structure-function relationships of *N*-ε-methylation of lysyl residues, the position of methylated residues in the sequence of *Ssβ*gly was determined (Table I and Fig. 5*A*), by a combination of chemical and enzymatic proteolysis and mass spectrometry. Although the precise measurement of the relative abundances of the modified *versus* unmodified residues was not permitted by the technique employed, Lys^{135} and Lys^{332} appeared to be in a prevailingly methylated form, whereas the modification of all other lysyl residues was substoichiometric. The amino acid composition analysis of native β-glycosidase showed that the *N*-ε-methyllysine content was between 14 and 17% of the total lysine content. This percentage corresponded to about 3–4 modified lysyl residues per monomer, of 23, indicating a modification efficiency of about 70%.

It is worth mentioning that the modified lysyl residues and some of the surrounding regions were not conserved in the sequence and structure alignments with other mesophilic glycosidases belonging to glycosyl hydrolase family I, as indicated in our previous work on *Ssβ*gly mutants (43). As an example,

the large domain between residues 83 and 124, containing methylated Lys^{116} and close to methylated Lys^{135}, was present only in hyperthermophilic archaea. This domain appears to be involved in the thermal resistance of *Ss*βgly, by stabilizing the fold of contacting α-helices 178–193 and 229–251 toward thermal perturbation (43). These observations suggest a role for the methylation of lysyl residues, located in specific domains, in the thermal stabilization of the protein. Also in the comparative topological analysis of *Ss*βgly and *Ss*ADH, the proximity to specific structural motifs (α-helices and β-turns bridging β-strands) appeared to be more relevant for methylation than simple physical parameters, such as the percentage of surface solvent accessibility.

A common characteristic of the sequence stretches not conserved in the mesophilic counterparts of thermophilic enzymes is a high concentration of charged residues (17, 22, 43). The role of ionic interactions, and especially their networks, in determining the increased thermal stability of several thermophilic proteins is well documented (44–50). Complex ionic interactions (51) are especially capable of enhancing stability through a cooperative strengthening mechanism (52). Theoretical models (53) show that salt bridges are preferentially stabilized at high temperatures, since the desolvation penalty in the association of two charged residues to form a salt bridge is markedly reduced. Holding these observations in due consideration, a stabilizing effect of methylated lysines could be explained by the capability of the methyl group, linked to the ϵ-amino group of lysine, to act as an electron inducer. Such behavior, in turn, should increase the pK_a of methylated lysyl residues and stabilize the partial positive charges of their side chain nitrogen atoms, thus creating stronger ionic interactions, as compared with unmethylated lysyl residues. In keeping with these considerations, all of the modified lysyl residues were involved in hydrogen bonds and ionic interactions with charged groups (Fig. 5*B*). Moreover, energy minimization calculations showed a general increase in the number of hydrogen bonds and a reduction of molecular distances between methyl-lysines and negatively charged groups (Fig. 5*B*). As a whole, these modifications are consistent with a more compact protein globule, with increased bonding stability and fewer energetic states. These implications provide a rationale, also, for our observation of the higher susceptibility of *Ec*Ssβgly to the dissociating action of SDS (Fig. 3). We have recently documented that a highly organized polar interaction network is responsible for the stabilization of *Ss*βgly toward SDS. It is evident that *N*-ϵ-methyl groups are essential for the formation of an extended network of ionic interactions, which is responsible for the enhanced resistance of the enzyme to various perturbants.

Conclusions—Post-translational modifications represent an important maturation step of proteins, which deeply affects their physico-chemical and biological properties, such as solubility, stability, enzymatic activity, and immunogenicity. The results of the present study document that *N*-ϵ-methylation of specific lysyl residues of β-glycosidase from *S. solfataricus* is associated with increased stability toward high temperature and SDS as well as a lower susceptibility to denaturation and aggregation, particularly at the high temperatures (>85 °C) typical of the natural environment of the organism (31). Such findings are particularly interesting, in light of recent observations collected with amyloid peptide β-(25–35), which is the shortest synthetic peptide retaining the β-sheet fibril-forming capability and toxicity of β-amyloid, the peptide believed to cause Alzheimer's disease. *N*-Methylation of amyloid peptide β-(25–35) prevented the aggregation and inhibited the resulting toxicity of the wild type peptide (11). Thus, similar effects seem to derive from a post-translational modification naturally evolved under extreme conditions, and a chemical strategy devised in order to counteract the effects of an altered protein processing. This suggests that the study of methylation, as well as other factors of protein stabilization toward extreme perturbations, may yield potentially useful information in regard to a number of pathological conditions associated with altered protein stability and aggregation.

REFERENCES

1. Paik, W. K., and Kim, S. (1986) *Yonsei Med. J.* **27,** 159–177
2. Dillon, N., and Festenstein, R. (2002) *Trends Genet.* **18,** 252–258
3. Rea, S., Eisenhaber, F., O'Carroll, D., Strahl, B. D., Sun, Z. W., Schmid, M., Opravil, S., Mechtler, K., Ponting, C. P., Allis, C. D., and Jenuwein, T. (2000) *Nature* **406,** 593–599
4. Czermin, B., Schotta, G., Hulsmann, B. B., Brehm, A., Becker, P. B., Reuter, G., and Imhof, A. (2001) *EMBO Rep.* **2,** 915–919
5. Lachner, M., O'Carroll, D., Rea, S., Mechtler, K., and Jenuwein, T. (2001) *Nature* **410,** 116–120
6. Bannister, A. J., Zegerman, P., Partridge, J. F., Miska, E. A., Thomas, J. O., Allshire, R. C., and Kouzarides, T. (2001) *Nature* **410,** 120–124
7. Nielsen, A. L., Oulad-Abdelghani, M., Ortiz, J. A., Remboutsika, E., Chambon, P., Losson, R. (2001) *Mol. Cell* **7,** 729–739
8. Tamaru, H., and Selker, E. U. (2001) *Nature* **414,** 277–283
9. Williamson, N. A., Raliegh, J., Morrice, N. A., and Wettenhall, R. E. (1997) *Eur. J. Biochem.* **246,** 786–793
10. Katz, M. L., Siakotos, A. N., Gao, Q., Freiha, B., and Chin, D. T. (1997) *Biochim. Biophys. Acta* **1361,** 66–74
11. Hughes, E., Burke, R. M., and Doig, A. J. (2000) *J. Biol. Chem.* **275,** 25109–25115
12. Minami, Y., Wakabayashi, S., Wada, K., Matsubara, H., Kerscher, L., and Oesterhelt, D. (1985) *J. Biochem.* (*Tokyo*) **97,** 745–753
13. Ammendola, B., Raia, C. A., Caruso, C., Camardella, L., D'Auria, S., De Rosa, M., and Rossi, M. (1992) *Biochemistry* **31,** 12514–12523
14. Maras, B., Consalvi, V., Chiaraluce, R., Politi, L., De Rosa, M., Bossa, F., Scandurra, R., and Barra, D. (1992) *Eur. J. Biochem.* **203,** 81–87
15. Zappacosta, F., Sannia, G., Savoy, L. A., Marino, G., and Pucci, P. (1994) *Eur. J. Biochem.* **222,** 761–767
16. Torchilin, V. P., Maksimenko, A. V., Smirnov, V. N., Klibanov, A. M., and Martinek, K. (1979) *Biochim. Biophys. Acta* **567,** 1–11
17. Gentile, F., Amodeo, P., Febbraio, F., Picaro, F., Motta, A., Formisano, S., and Nucci, R. (2002) *J. Biol. Chem.* **277,** 44050–44060
18. Moracci, M., Nucci, R., Febbraio, F., Vaccaro, C., Vespa, N., La Cara, F., and Rossi, M. (1995) *Enzyme Microb. Technol.* **17,** 992–997
19. Cacace, M. G., De Rosa, M., and Gambacorta, A. (1976) *Biochemistry* **15,** 1692–1696
20. Nucci, R., Moracci, M., Vaccaro, C., Vespa, N., and Rossi, M. (1993) *Biotechnol. Appl. Biochem.* **17,** 239–250
21. Salomaa, P., Schaleger, L. L., and Long, F. A. (1964) *J. Am. Chem. Soc.* **86,** 1–7
22. Aguilar, C. F., Sanderson, I., Moracci, M., Ciaramella, M., Nucci, R., Rossi, M., and Pearl, L. H. (1997) *J. Mol. Biol.* **271,** 789–802
23. Biosym/MSI (1995) *InsightII User Guide*, Biosym/MSI, San Diego, CA
24. Koradi, R., Billeter, M., and Wûthrich, K. (1996) *J. Mol. Graphics* **14,** 51–55
25. Cubellis, M. V., Rozzo, C., Montecucchi, P., and Rossi, M. (1990) *Gene* (*Amst.*) **94,** 89–94
26. Cubellis, M. V., Rozzo, C., Nitti, G., Arnone, M. I., Marino, G., and Sannia, G. (1989) *Eur. J. Biochem.* **186,** 375–381
27. Thompson, J. D., Higgins, D. G., and Gibson, T. J. (1994) *Nucleic Acids Res.* **22,** 4673–4680
28. Esposito, L., Sica, F., Raia, C. A., Giordano, A., Rossi, M., Mazzarella, L., Zagari A. (2002) J. *Mol. Biol.* **318,** 463–477
29. Guex, N., and Peitsch, M. C. (1997) *Electrophoresis* **18,** 2714–2723
30. Westhead, D. R., Slidel, T. W. F., Flores, T. P. J., and Thornton, J. M. (1999) *Protein Sci.* **8,** 897–904
31. De Rosa, M., Gambacorta, A., Nicolaus, B., Buonocore, V., and Poerio, E. (1980) *Biotechnol. Lett.* **2,** 29–34
32. Skorko-Glonek, J., Lipinska, B., Krzewski, K., Zolese, G., Bertoli, E., and Tanfani, F. (1997) *J. Biol. Chem.* **272,** 8974–8982
33. Fernandez-Ballester, G., Castresana, J., Arrondo, J. L. R., Ferragut, L. A., and Gonzales-Ros, J. M. (1992) *Biochem. J.* **288,** 421–426
34. Banecki, B., Zylicz, M., Bertoli, E., and Tanfani, F. (1992) *J. Biol. Chem.* **267,** 25051–25058
35. Tanfani, F., Bertoli, E., Signorini, M., and Bergamini, C. M. (1993) *Eur. J. Biochem.* **218,** 499–505
36. Osborne, H. B., and Nabedryk-Viala, E. (1982) *Methods Enzymol.* **88,** 676–680
37. Umemara, J., Cameron, D. G., and Mantsch, H. H. (1980) *Biochim. Biophys. Acta* **602,** 32–44
38. Sackett, D. L., and Wolff, J. (1987) *Anal. Biochem.* **167,** 228–234
39. Laemmli, U. K. (1970) *Nature* **227,** 680–685
40. Lindo, V. S., Kakkar, V. V., Learmonth, M., Melissari, E., Zappacosta, F., Panico, M., and Morris, H. R. (1995) *Br. J. Haematol.* **89,** 589–601
41. Haseltine, C., Montalvo-Rodriguez, R., Bini, E., Carl, A., and Blum, P. (1999) *J. Bacteriol.* **181,** 3920–3927
42. Fontana, A. (1991) in *Life under Extreme Conditions* (Di Prisco, G., ed) pp. 89–113, Springer-Verlag, Berlin
43. Bismuto, E., Febbraio, F., Limongelli, S., Briante, R., and Nucci R. (2003) *Proteins Struct. Funct. Genet.* **51,** 10–20
44. Walker, J. E., Wonacott, A. J., and Harris, J. I. (1980) *Eur. J. Biochem.* **108,**

581–586
45. Chan, M. K., Mukund, S., Kletzin, A., Adams, M. W., and Rees, D. C. (1995) *Science* **267,** 1463–1469
46. Korndörfer, I., Steipe, B., Huber, R., Tomschy, A., and Jaenicke, R. (1995) *J. Mol. Biol.* **246,** 511–521
47. Tomschy, A., Böhm, G., and Jaenicke, R. (1994) *Protein. Eng.* **7,** 1471–1478
48. Kelly, C. A., Nishiyama, M., Ohnishi, Y., Beppu, T., and Birktoft, J. J. (1993) *Biochemistry* **32,** 3913–3922
49. Spassov, V. Z., Karshikoff, A. D., and Ladenstein, R. (1995) *Protein Sci.* **4,** 1516–1527
50. Vogt, G., Woell, S., and Argos, P. (1997) *J. Mol. Biol.* **269,** 631–643
51. Musafia, B., Buchner, V., and Arad, D. (1995) *J. Mol. Biol.* **254,** 761–770
52. Horovitz, A., Serrano, L., Avron, B., Bycroft, M., and Fersht, A. R. (1990) *J. Mol. Biol.* **216,** 1031–1044
53. Elcock, A. H. (1998) *J. Mol. Biol.* **284,** 489–502
54. Humphrey, W., Dalke, A., and Schulten, K. (1996) *J. Mol. Graphics* **14,** 33–38